Evaluatins Impact Factor IBGM 2017 – 2018
IRAQI BULLETIN OF GEOLOGY AND MINING
Arcif: 0.0755
GIF: 0.936

Iraqi Bulletin of Geology and Mining *Vol.15, No.1, 2019* *p 43 – 57*

PALEOSTRESS ANALYSIS OF NEOGENE ROCKS IN ZURBATIYAH AREA, E IRAQ

Ali Kh. Al-Shwaily[1] and Mostafa R. Al-Obaidi[2]

Received: 02/ 04/ 2018, Accepted: 16/ 08/ 2018
Key words: Paleostress; Stress inversion; Stress tensor; Zurbatiyah; Low Folded Zone; Iraq

ABSTRACT

Faults of Neogene age in the Zurbatia area have been analysed in the light of Anderson faulting theory, Jaeger reactivated assumption and plate tectonic theory to derive the mechanism style and paleostress systems prevailing in the study area. According to the graphical methods (improved right dihedral and rotational optimization methods), the NE – SW compressive force of the Oligocene changed later in Late Miocene age into E – W compression. This study suggests, that the area is affected by gradual change in stress regime from NE – SW very high compressional phase of faulting to very low compressional phase. The NE – SW and E – W directed pressure is presumably identical with the northeasterly driving motion of the Arabian Plate.

تحليل الآجهاد القديم لصخور عمر النيوجين في منطقة زرباطية، شرق العراق

علي خضير الشويلي ومصطفى رشيد العبيدي

المستخلص

تم تحليل الفوالق الموجودة في صخور عمر النيوجين في منطقة زرباطية على ضوء نظرية اندرسون للتصدع، فرضية جاكير لإعادة التنشيط ونظرية حركة الصفائح لمعرفة أنظمة الإجهادات القديمة السائدة في منطقة الدراسة وذلك باستخدام طريقة الأوجه الثنائية المتعامدة وطريقة التحسين الدورية، حيث ان القوة الضغطية ذات الاتجاه شمال شرق – جنوب غرب في عمر الأوليغوسين قد تغيرت الى قوة ضغطية ذات اتجاه شرق – غرب في عمر المايوسين المتاخر. تقترح هذه الدراسة ان منطقة الدراسة قد تعرضت الى تغير تدريجي في نظام الإجهاد من طور تصدع ذو شدة عالية جدا باتجاه شمال شرق – جنوب غرب الى طور ضغطي واطيء الشدة وان اتجاهات الاجهادات في منطقة الدراسة مطابقة الى الحركة الشمالية الشرقية للصفيحه العربية.

INTRODUCTION

Analyses of brittle structures provide a reliable key to understand the distribution and evolution of paleostress fields through successive tectonic events. Paleostresses analysis refers to various methods which attempt to determine a regional stress tensor consistent with existing geological structures. Several different techniques for estimating stress tensors have been proposed. The principal stress directions and relative magnitudes have been determined from fault populations (Angelier and Mechler, 1977). The determination of the paleo- or present-day stress field is important to understand regional deformation events and natural hazard assessment. The stress analysis allows users to quickly identify structures at risk of

[1] Iraq Geological Survey; on a postgraduate study-leave at the College Science, Univesrsity of Baghdad, e-mail: Ali.kh.geosurv@gmail.com
[2] Department of Earth Sciences, College of Science, University of Baghdad, Iraq.

reactivation and failure. The assessment of fault and fracture reactivation is vital in the management of reservoir, mining and other engineering sectors (Igwe and Okonkwo, 2016).

Recovering the paleostress field from observed fault slip data have been developed over the last five decades. These methods are based on the Wallace (1951) and Bott (1959) assumption suggesting that slip direction is parallel to the resolved shear stress on the fault plane (Angelier, 1979; Aydin, 1980; Etchecopar *et al*., 1981; Angelier *et al*., 1982; Angelier, 1984; Michael, 1984; Aleksandrowski, 1985; Angelier, 1985; Angelier *et al*., 1985; Frizzell and Zoback, 1987; Hancock *et al*., 1987; Julien and Cornet, 1987; Lisle, 1987; Pfiffner and Burkhard, 1987; Reches, 1987; Sassi and Carey-Gailhardis, 1987; Caputo and Caputo, 1988; Célérier, 1988; Larroque and Laurent, 1988; Lisle, 1988; Angelier, 1989; Hardcastle, 1989; Hatzor and Reches, 1990; Manning and de Boer, 1989; Wallbrecher and Fritz, 1989). The aim of this paper is to determine the tectonic and the orientation of the paleostresses that affected the study area and to reconstruct their stress map and stress trajectories via using the inversion methods.

GEOLOGICAL SETTING

The study area is located within the eastern part of Wasit Governorate, along the Iraqi-Iranian international borders. It occupies, approximately, an area of 700 Km^2 (Fig.1). The main towns in the study area are Badrah, Zurbatiyah and Jassan. It is limited by the following coordinates:

Longitudes	45° 52' 45" E	46° 07' 45" E
Latitudes	33° 07' 35" N	33° 22' 37" N

▪ Geomorphology

The study area represents the extreme margin of the Low Folded Zone, which is physiographically, known as the Foothill Zone, located between High Mountain and Mesopotamian Plain provinces of Iraq (Yacoub *et al*., 2012). From topographic point of view, the study area descends in relief from its NE part, where the mountainous area exists, towards W and SW parts, where alluvial fans and sheet run off areas are well developed (Mahmoud *et al*., 2018).

▪ Lithostratigraphy

Different lithological units of sedimentary origin crop out across the study area, they range from Oligocene (Ibrahim Formation), to Bai Hassan Formation (Pliocene – Pleistocene) with various types of Quaternary sediments (Fig.1). Brief description of the lithological units is hereinafter:

– **Ibrahim Formation (Oligocene):** It is exposed within the eastern part of the study area and represents the oldest rock unit within the hanging wall of Koolic thrust fault, which is thrusted on Dhiban and Jeribe formations (foot wall), it consists of 130 m of alternation of marl and marly limestone, The upper part of the formation is dominated by marl with thin beds of limestone while the middle part is composed of thickly bedded marly limestone and alternation of marly limestone and marl in the lower part (Mahmoud *et al*., 2018).

– **Serikagni Formation (Lower Miocene):** It is exposed in the eastern parts of the study area and consists of 22 m of marl, marly limestone and limestone.

– **Dhiban Formation (Lower Miocene):** It exists within in the eastern parts of the study area and consists of 30 m of white nodular and massive gypsum.

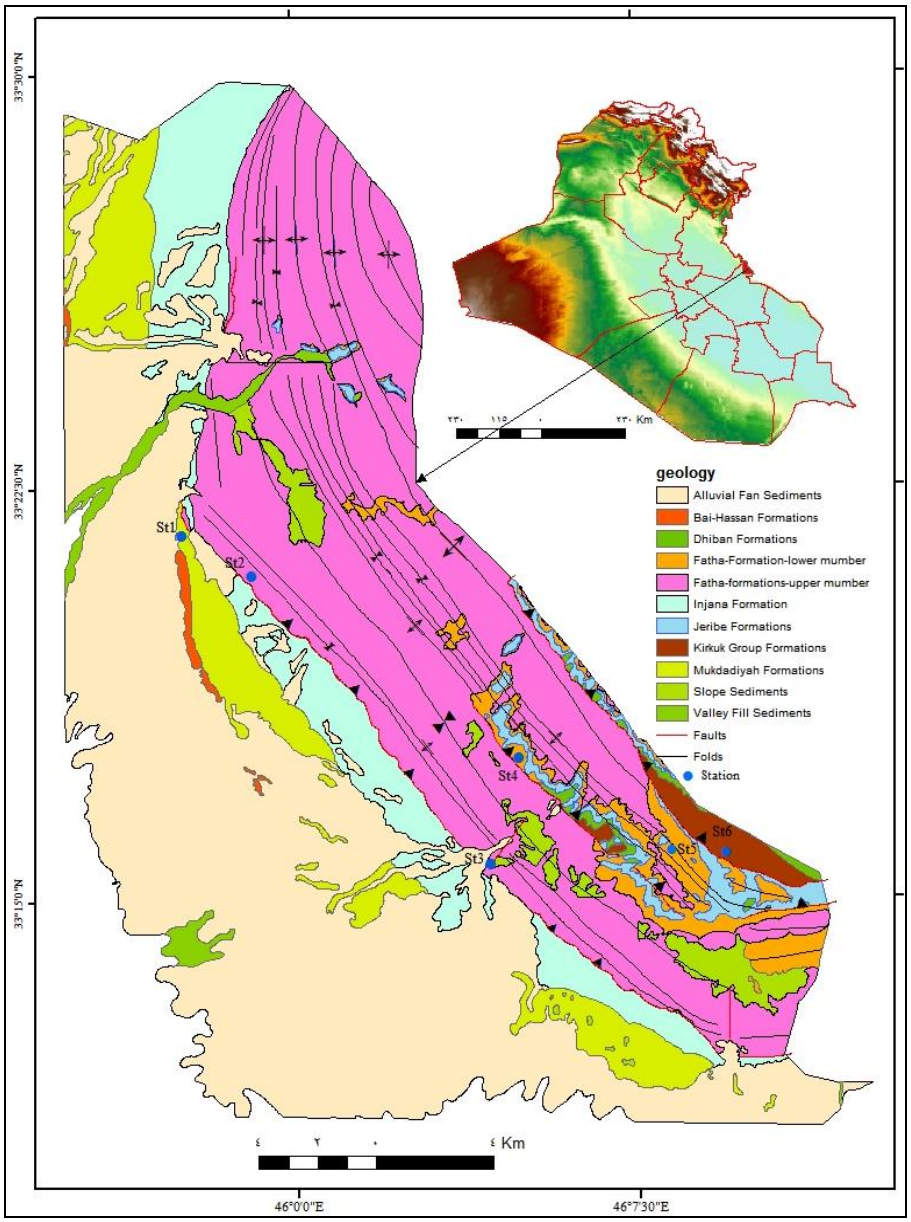

Fig.1: Location and geological map of the study area (Mahmoud *et al*., 2018)

– **Jeribe Formation (Middle Miocene):** It is comprised of 70 m of massive dolomitic limestone.

– **Fat'ha Formation (Middle Miocene):** The formation consists of cyclic alternation of calcareous claystone, limestone and gypsum. It is divided into two members (Al-Mubarak and Youkhanna, 1976 and Ma'ala *et al*., 1987), both members are exposed in the study area. The maximum exposed thickness of the formation is 330 m. The Fat'ha Formation is thrusted over Injana Formation along the major thrust fault.

– **Formation (Upper Miocene):** The formation is exposed only within south western limb of Hemrin anticline, Injana formation consists of alternation of claystone and sandstone**,** The uppermost part is characterized by very thick (up to 30 m) claystone and thin sandstone beds. The total thickness is 350 m.

– **Mukdadiyah Formation (Upper Miocene-Pliocene):** It consists of 110 m of rhythmic clastic cycles of lenticular sandstone and claystone, with many lateral changes.

– **Bai Hassan Formation (Pliocene – Pleistocene):** The formation consists of thick and coarse conglomerates contain lenses of sandstones. The total exposed thickness is 25 m (Mahmoud *et al*., 2018).

- **Structural elements**

The study area is located in the Low Folded Zone of Iraq. It is part of the Zagros Fold Thrust Belt in the Iraqi territory, which is divided into several NW – SE trending longitudinal tectonic zones (Buday and Jassim, 1987; Al-Kadhimi *et al*., 1996; Jassim and Goff, 2006 and Fouad, 2012). The Low Folded Zone is considered part of the Outer Platform of the Arabian Plate by Fouad (2012). The main structural elements reported in the study area are:

– **Hemrin anticline:** It is the major structure within the study area, it is NNW – SSE trending anticline, 33 Km in length and its width ranges from 0.7 Km up to 7 Km. the NE limb of Hemrin anticline is thrust over its SW limb.

– **Kani Sakht anticline:** It is a narrow asymmetrical fold, located along the eastern side of the Hemrin structure, with length of about 30 Km and variable width of up to 1.5 Km. It has a NWN – SES trend. The dip of the southwestern limb is about (40 – 65) degrees, whereas the dip of the northeast limb is about (47 – 52) degree.

– **Faults:** The study area is characterized by the development of three large scale thrust faults of NW – SE trend, Kachaa Fault extends for 25 Km, Cea Koran Fault extends for 25 Km in length, Koolic Fault, it runs parallel to the Iraqi – Iranian international borders, extends for 12 Km in length.

METHODOLOGY

- **Assumptions and theories**

In a rock body under stress, slip can occur on pre-existing zones of weakness in a variety of orientations relative to the principal stresses (Al-Kotbah and Al-Ubaidi, 2001).

– **Anderson faults:** Dynamic analysis of fault system (Anderson, 1942) is based on the assumption of simple relationship between conjugate brittle shear and the principal axes of the stress responsible for their formation. The orientation of fault planes is used directly to interpret the principal stress directions. The movement vector is assumed to be normal to the intersection of the conjugate pair.

– **Reactive faults:** According to the theory of Jagaer (1969), within a rock body containing a multitude of fracture discontinuities, the superimposition of a stress may result in movement on several sets of faults. According to Bott (1959), faults may frequently arise from the existence of old planes of fractures within the rock (Al-Ubaidi and Al-Kotbah, 2003).

– **Plate Tectonics:** Plate tectonic theory explains crustal movements and evolution. The idea of plate tectonic arose from the observation that large areas of the Earth's crust have suffered very little distortion although they travelled laterally several kilometers (Park, 1997). The Arabian Plate experienced nearly NE – SW trending tensional stress from Triassic to early Cretaceous, which became strongly compressional towards Late Cretaceous (Marzouk and Sattar, 1994). From Cenozoic time, the maximum principal horizontal stress remained compressional with NE – SW direction due to the relative movement of the Arabian Plate.

- **Paleostress inversion methods**

The most common and extensively used method of stress inversion typically involves use of faults with slickenlines that record the direction of slip relative to the fault plane (Hancock, 1985; Angelier 1994; Ramsay and Lisle, 2000). Their use is based on the Wallace-Bott hypothesis which states that the slip on a planar structure is assumed to occur parallel to the greatest resolved shear stress (Bott, 1959). Determining the reduced stress tensor is considered as the main goal of stress inversion, the four parameters of the reduced stress tensor are maximum principal stress axis (σ1), intermediate stress axis (σ2), minimum stress axis (σ3) and stress ratio (R).

- **Method of work**

The fault kinematic data are collected from six stations, distributed across the study area, the area sampled is kept small enough (1000 – 2500 m^2) in order to guarantee homogeneity of results (Delvaux and Sperner, 2003). In order to compute and analyse the field data, TENSOR WIN software is used (Delvaux, 1993; Delvaux *et al*., 1997; Delvaux and Sperner, 2003). This program is a tool for controlled interactive separation of fault slip or focal mechanism data and progressive stress tensor optimization using successively the Right Dihedron method and the Rotational Optimization method.

RESULTS

- **Station 1**

The measurements of this station were collected from claystone and sandstone beds along a major stream meander, flows within the Injana Formation. The faults of this station are of reverse sense (Table 1). The reduced stress tensor (σ1, σ2, σ3), stress ratio (R) and stress index, obtained from the whole fault population of this station, are: σ1 = 04/265, σ2 = 14/174, σ3 = 76/011 and R = 0.52, which indicate pure ENE – WSW compressive stress regime (Fig.2).

- **Station 2**

This station is located within the thrust front of the major thrust fault, where the Fat'ha Formation is thrusted over the Injana Formation. The collected measurements of this station are taken from gypsum and limestone beds of the Fat'ha Formation, where all the faults are of thrust and reverse types. Eleven fault planes with their slickensides are measured within this station and later used in computation (Table 2). The reduced stress tensor parameters, obtained from the whole fault population of this station, are the following: σ1= 07/225, σ2 = 21/132, σ3 = 68/332 and R = 0.64, which indicate NE – SW maximum shortening and NW – SE extension which is a pure compressive tensor. The stress index (R`) of this station = 2.64 based on right dihedral method and rotational optimization methods, respectively, which indicates a pure compressive stress regime (Fig.3).

- **Station 3**

This station is located within the thrust front of the major thrust fault in the study area, where the Fat'ha Formation (Middle Miocene) is thrusted over the Injana Formation (Upper Miocene). The collected measurements of this station are taken from gypsum and limestone beds of the Fat'ha Formation and where all the faults are of thrust and reverse types (Table 3). The reduced stress tensor parameters, which are obtained from the whole fault population of this station, are: σ1= 15/026, σ2 = 11/119, σ3 = 71/245 and R = 0.76, which indicates NNE – SSW compression and WNW – ESE extension, which is a radial compressive tensor and the stress index (R`) of this station = 2.76 (Fig.4).

Table 1: Field measurements of Station 1

No	Fault type	Dip Direction	Dip amount	Pole	Pitch amount
1	Thrust fault	220°	80°	040°/10°	85° NW
2	Thrust fault	225°	81°	045°/9°	88° NW
3	Thrust fault	231°	83°	051°/7°	84° NW
4	Thrust fault	218°	80°	042°/10°	75° NW
5	Thrust fault	213°	81°	033°/9°	85° NW
6	Thrust fault	057°	79°	237°/11°	70° SE
7	Thrust fault	058°	79°	236°/11°	81° SE
8	Thrust fault	062°	77°	242°/13°	83° SE
9	Thrust fault	067°	53°	247°/37°	72° SE
10	Thrust fault	067°	53°	247°/37°	89° SE
11	Thrust fault	058°	86°	238°/4°	85° SE
12	Thrust fault	240°	76°	060°/14°	75° NW
13	Thrust fault	051°	88°	231°/2°	70° SE
14	Thrust fault	225°	78°	045°/12°	85° SE
15	Thrust fault	210°	70°	030°/20°	70° NW

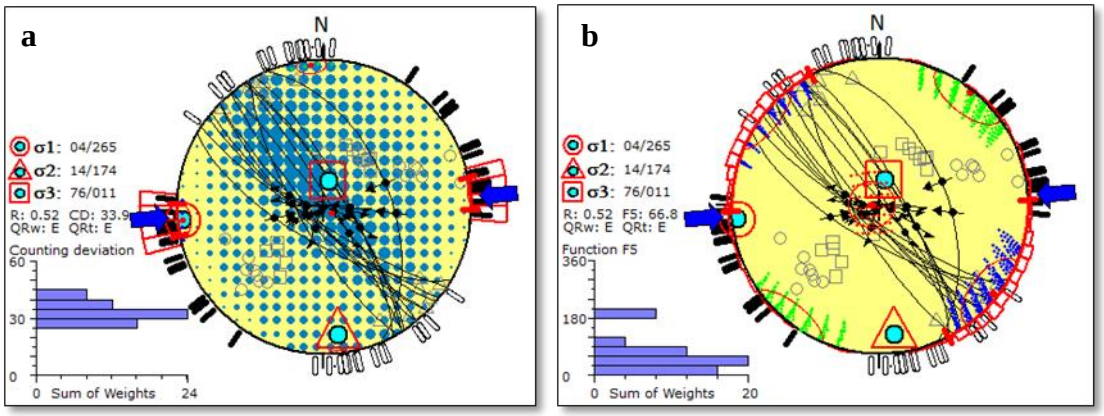

Fig.2: Stereographic projection of Station 1: **a)** right dihedral method and; **b)** rotational optimization method

Table 2: Field measurements of Station 2

No	Fault type	Dip Direction	Dip amount	Pole	Pitch amount
1	Thrust fault	044°	24°	224/66°	60° W
2	Thrust fault	088°	58°	268/32°	55° N
3	Thrust fault	225°	38°	045/52°	85° W
4	Thrust fault	215°	45°	035/65°	75° W
5	Thrust fault	062°	46°	242/44°	70° W
6	Thrust fault	068°	50°	248/40°	70° W
7	Thrust fault	230°	60°	050/30°	75° W
8	Thrust fault	210°	55°	030/35°	60° W
9	Thrust fault	216°	65°	036/25°	80° W
10	Thrust fault	054°	50°	234/40°	58° N
11	Thrust fault	048°	40°	228/50°	60° N

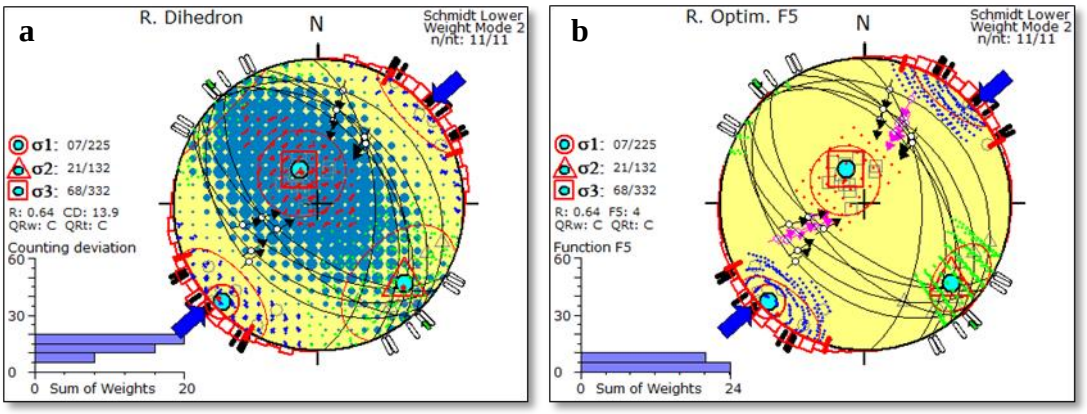

Fig.3: Stereographic projection of Station 2: **a)** right dihedral method; **b)** rotational optimization method

Table 3: Field measurements of station 3

No	Fault type	Dip Direction	Dip amount	Pole	Pitch amount
1	Thrust fault	045°	75°	225°/15°	75° N
2	Thrust fault	128°	75°	308°/15°	25° S
3	Thrust fault	038°	74°	218°/16°	70° N
4	Thrust fault	038°	78°	218°/12°	72° N
5	Thrust fault	067°	44°	247°/46°	75° N
6	Thrust fault	067°	44°	247/46°	60° S
7	Thrust fault	068°	44°	248°/46°	55° N
8	Thrust fault	058°	60°	238°/30°	88° S
9	Thrust fault	029°	48°	209°/42°	78° S
10	Thrust fault	025°	23°	205°/67°	70° N
11	Thrust fault	074°	43°	254°/47°	70° N
12	Thrust fault	120°	60°	300°/30°	52° S
13	Thrust fault	060°	58°	240°/32°	70° N
14	Thrust fault	135°	45°	315°/45°	60° S

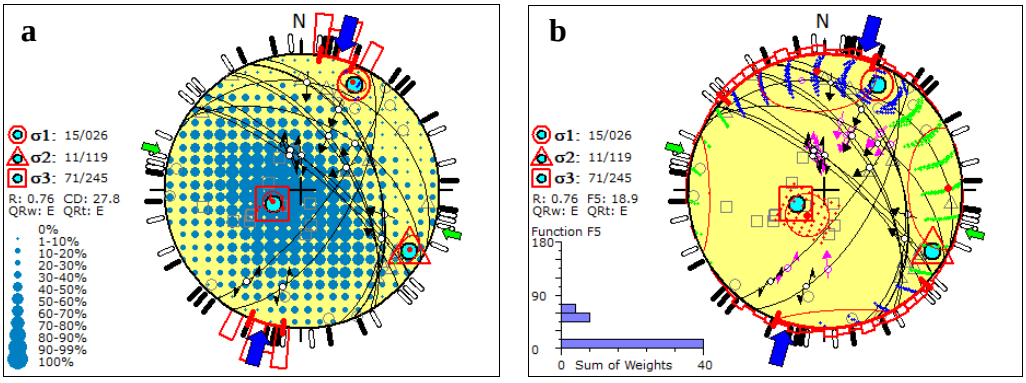

Fig.4: Stereographic projection of Station 3: **a)** right dihedral method; **b)** rotational optimization method

- **Station 4**

This station is located within the NE limb of Hemrin South anticline in the Zurbatiyah area, within a road cut, where the Jeribe Formation (Lower Miocene) is exposed. All the faults are of thrust and reverse types, ten fault planes with their slickensides are measured within this station and later used in computation (Table 4). The reduced stress tensor parameters (σ1, σ2, σ3 and stress ratio), which are obtained from the whole fault population of this station are: σ1 = 17/195, σ2 = 28/096, σ3 = 57/313 and R = 0.44, which indicates a pure compressive tensor of NNE – SSW compression and WNW – ESE extension, whereas the stress index (R`) of this station = 2.44 based on right dihedral method and rotational optimization methods, respectively, which indicates a compressive stress regime (Fig.5).

Table 4: Field measurements of Station 4

No	Fault type	Dip direction	Dip amount	Pole	Pitch amount
1	Thrust fault	012°	38°	192°/52°	75°
2	Thrust fault	187°	90°	077°/0°	60°
3	Thrust fault	175°	90°	355°/0°	80°
4	Thrust fault	185°	88°	005°/2°	70°
5	Thrust fault	180°	64°	000°/26°	88°
6	Thrust fault	008°	45°	188°/45°	64°
7	Thrust fault	188°	85°	008°/5°	75°
8	Thrust fault	035°	60°	215°/30°	80°
9	Thrust fault	072°	88°	252°/2°	88°
10	Thrust fault	020°	40°	200°/50°	60°

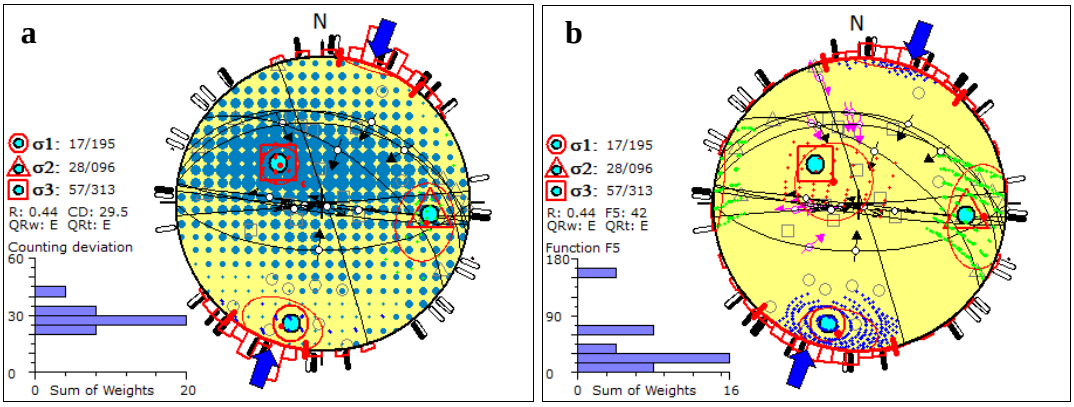

Fig.5: Stereographic projection of Station 4: **a)** right dihedral method;
b) rotational optimization method

- **Station 5**

This station is located within Kollak thrust fault in the Zurbatiyah area, where the Ibrahim Formation is thrusted over the Dhiban Formation. The collected measurements of this station are taken from the limestone beds of the Ibrahim Formation and all the faults, within this station, are of thrust and reverse types. Thirteen fault planes with their slickensides are measured within this station and later used in computation (Table 5). The reduced stress tensor parameters (σ1, σ2, σ3 and stress ratio), obtained from the whole fault population are: σ1 = 05/041, σ2 = 29/308, σ3 = 60/139 and R = 0.35, which indicate a pure compressive tensor of NE – SW compression and NW – SE extension (Fig.6), whereas the stress index

(R`) of this station = 2.35 based on right dihedral method and rotational optimization methods respectively, that indicates a compressive stress regime (σ3 is vertical, 0.25 < R > 0.75).

- **Station 6**

This station is located within the Koolic thrust fault, where the Ibrahim Formation is thrusted over the Dhiban Formation. The collected measurements of this station are taken from the limestone beds of the Ibrahim Formation and all the faults within this station are of thrust and reverse types. Thirteen fault planes with their slickensides are measured within this station and later used in computation (Table 6). The reduced stress tensor parameters (σ1, σ2, σ3 and stress ratio R), obtained from the whole fault population, are: σ1= 02/025, σ2 = 21/294, σ3 = 69/119 and R = 0.75 and these stress parameters indicate a compressive tensor of radial compressive regime (σ3 is vertical, 75< R > 1) with NNE – SSW compression and WNW – ESE extension, whereas the stress index (R`) of this station = 2.75 (Fig.7).

Table 5: Field measurements of station 5

No	Fault type	Dip direction	Dip amount	Pole	Pitch amount
1	Thrust fault	038°	58°	218°/32°	77° NW
2	Thrust fault	038°	58°	218°/32°	70° NW
3	Thrust fault	222°	70°	042°/20°	75° SE
4	Thrust fault	218°	78°	038°/12°	80° SE
5	Thrust fault	042°	65°	222°/25°	88° NW
6	Thrust fault	021°	65°	201°/25°	75° SE
7	Thrust fault	040°	70°	220°/20°	80° NW
8	Thrust fault	228°	85°	048°/5°	74° NW
9	Thrust fault	020°	77°	200°/13°	82° NW
10	Thrust fault	030°	85°	210°/5°	74° NW
11	Thrust fault	030°	86°	210°/4°	80° SE
12	Thrust fault	210°	75°	030°/15°	65°NW
13	Thrust fault	215°	70°	035°/20°	70° NW

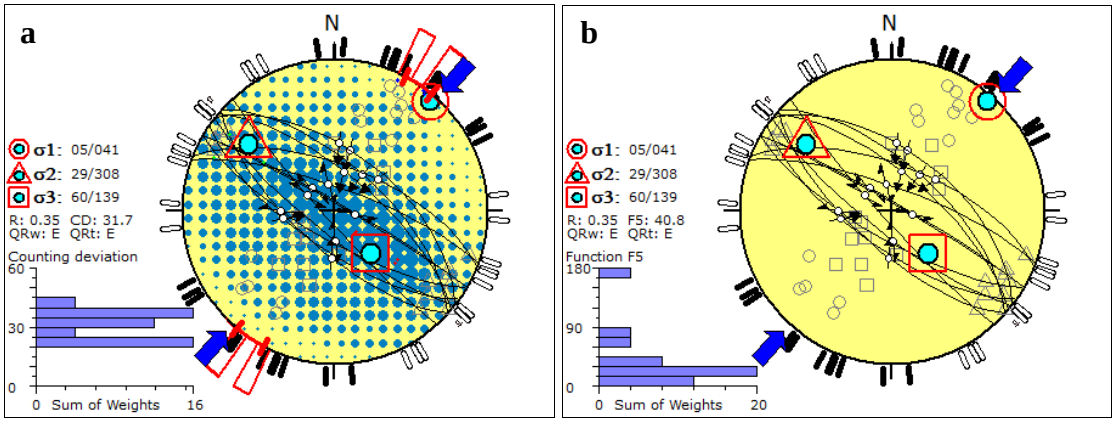

Fig.6: stereographic projection of station 5: **a)** right dihedral method;
b) rotational optimization method

Table 6: Field measurements of Station 6

No	Fault type	Dip direction	Dip amount	Pole	Pitch amount
1	Thrust fault	210	77	030°/13°	88 SE
2	Thrust fault	210	78	030°/12°	66 SE
3	Thrust fault	025	65	205°/25°	77 SE
4	Thrust fault	290	87	110°/3°	65 S
5	Thrust fault	320	70	140°/20°	85 S
6	Thrust fault	320	70	140°/20°	88 S
7	Thrust fault	214	80	034°/10°	85 S
8	Thrust fault	020	70	200°/20°	80 SE
9	Thrust fault	012	76	192°/14°	77 SE
10	Thrust fault	024	80	204°/10°	85 NW
11	Thrust fault	280	62	100°/28°	58 SE
12	Thrust fault	237	80	057°/10°	75 S
13	Thrust fault	040	60	220°/30°	58 NW

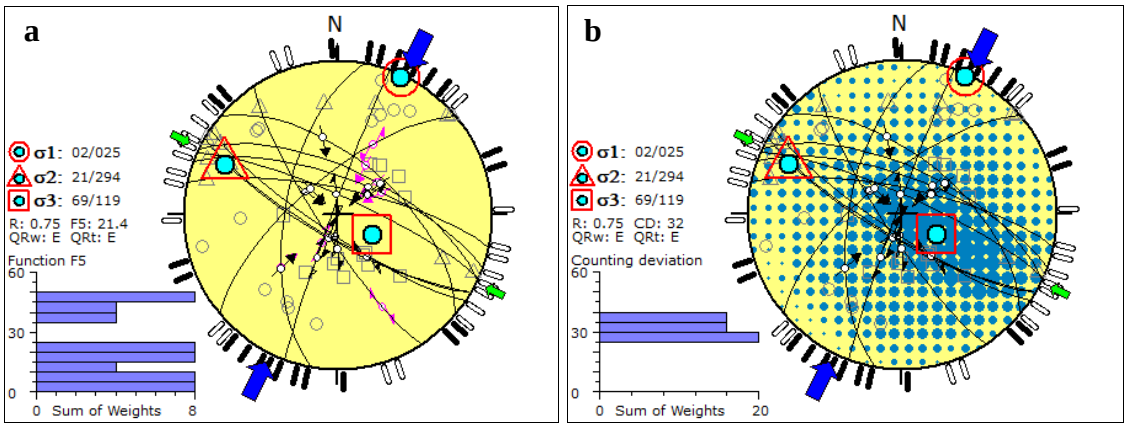

Fig.7: Stereographic projection of Station 6: **a)** right dihedral method; **b)** rotational optimization method

- **Stress Regime And Stress Map**

Depending on the nature of the vertical stress axes, the stress regime can be determined: it is extensional when σ1 is vertical, strike-slip when σ2 is vertical and compressional when σ3 is vertical (Anderson, 1951). The stress regimes also vary, within these three main types, as a function of the stress ratio (R): Radial extension (σ1 vertical, $0 < R < 0.25$), Pure extension (σ1 vertical, $0.25 < R < 0.75$), Transtension (σ2 vertical, $0.75 < R < 1$ or σ2 vertical, $1 > R > 0.75$), Pure strike-slip (σ2 vertical, $0.75 > R > 0.25$), Transpression (σ2 vertical, $0.25 > R > 0$ or σ3 vertical, $0 < R < 0.25$), Pure compression (σ3, vertical, $0.25 < R < 0.75$) and Radial compression (σ3 vertical, $0.75 < R < 1$) (Delvaux *et al*., 1997 and Delvaux and Sperner 2003). The type of stress regime can be expressed numerically using an index R', ranging from 0.0 to 3.0 and defined as follows (Fig.8):

R' = R when (σ1 is vertical; extensional stress regime)
R' = 2 – R when (σ2 is vertical; strike-slip stress regime)
R' = 2 + R when (σ3 is vertical; compressional stress regime)

The index R' defines the stress regime completely and is convenient for computing the mean regional stress regime from a series of individual stress tensors in a given area

(Benkhelil, 1989 and Igwe and Okonkwo, 2016). On structural maps, the stress tensors are displayed with the orientation of both horizontal principal stress (SHmax) and horizontal minimum stress axes (SHmin) as recommended by Guiraud *et al.* (1989). The horizontal stress is the dominant stress due to horizontal plate movement, mapping the azimuth of these axes is the best way to display the tectonic stress axes. Fig.9 shows types of stress tensors which have affected the study area.

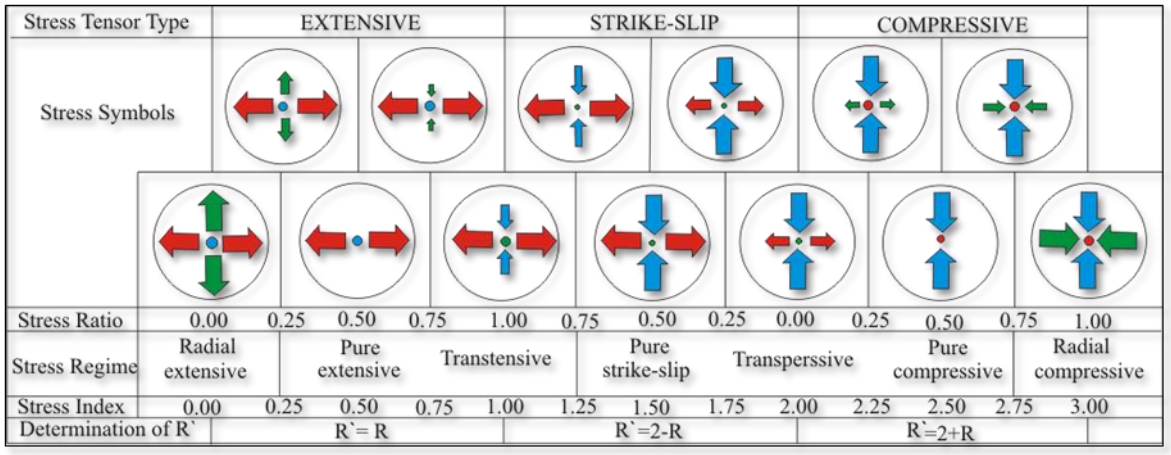

Fig.8: Stress tensor representation for different stress regimes
(after Guiraud *et al*., 1989)

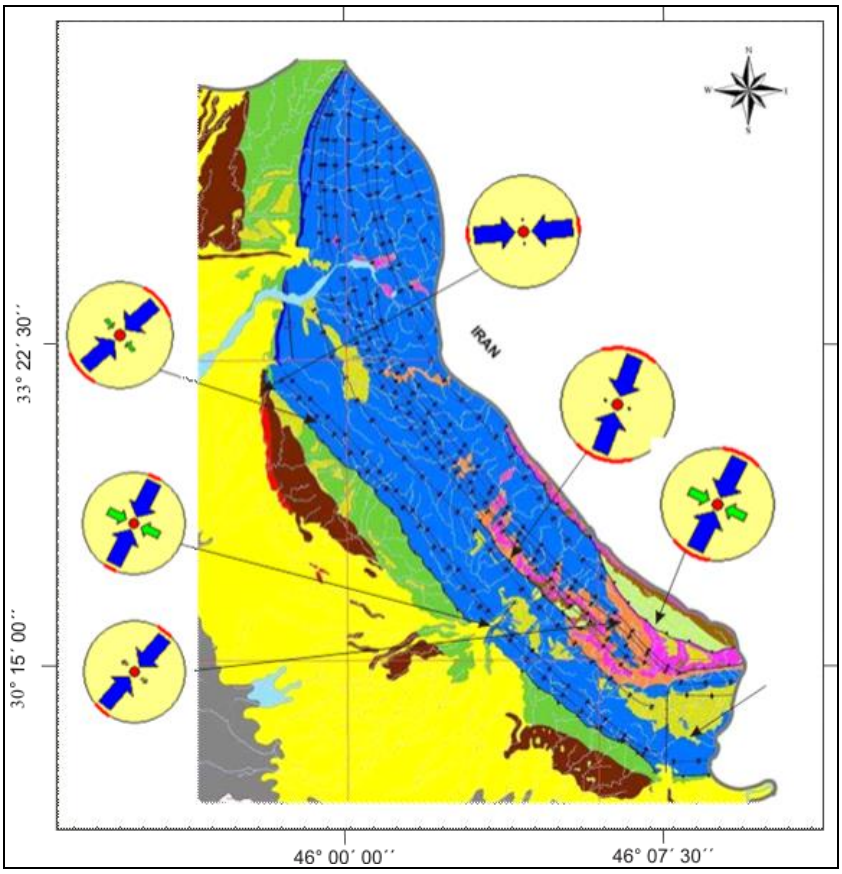

Fig.9: Shows the stress fields distribution, characterized by NE – SW compression and NW – SE extension in the study area

DISCUSSION

One of the most important issues in paleostress inversion studies is to date the constructed stress configurations. This may be achieved by dating the stratigraphical horizons involved in the faulting and the relationship between sedimentation and tectonics (Angelier, 1994). In this respect, syn-sedimentary structures provide invaluable information for the dating of constructed stress configurations.

To interpret results of paleostress analyses at the regional scale, it is necessary to compare paleostress reconstructions from numerous sites. A map of stress trajectories is thus drawn for a given tectonic event (Angelier, 1989).The fault kinematic data have been collected from different lithological units of different ages; from Ibrahim Formation (Oligocene) to Injana Formation (Upper Miocene), which show that the study area is influenced by NNE – SSW and NE – SW compressive stress tensors. The orientation of the maximum stress axis (σ1) ranges from 04/265 in Station one to 17/195 in Station four.

The obtained stress ratio (R) in Station one = 0.52; in Station two = 0.64; in Station three = 0.76; in Station four = 0.44; in station five = 0.44 and in station six = 0.75. The minimum principal stress axis (σ3) represents the vertical axis in all analyzed stations. According to the aforementioned data the resulted stress regime is a pure compressive tensor in stations one, two, four and five, whereas, it is radial compressive tensor in stations three and six.

Due to the horizontal and vertical orientations of Maximum Principal Stress Axis (σ1) and the Minimum Principal Stress Axis (σ3), the Stress Index (R`) is calculated, after applying equation (1), which refers to the numerical expression of the stress regime:

$$R` = 2 + R \quad \ldots\ldots\ldots\ldots\ldots\ldots \quad 1$$

The results show, that the value of the Stress Index (R`) in Station one = 2.52; in Station two = 2.64; in Station three = 2.76; in station four = 2.44 in Station five = 2.35 and in Station six = 2.75. All the calculated values indicate compressive stress regime.

The stress maps (Figs.9 and 10) show the study area was subjected to two main stress fields, the first is characterized by NE – SW and NNE – SSW compressions and NW – SE and WNW – ESE extensions, which continued from the Oligocene to the Middle Miocene and is recorded in stations 2,3,4,5 and 6, whereas the second stress field is characterized by E – W compression and N – S extension and is recorded in Station 1, which started in the Late Miocene. Moreover, the study area was subjected to two intense compressive forces; the first one is dated as Oligocene and the second within the Middle Miocene. Both of these stress fields belong to compression stress regime and oblique-slip, which means, the study area was subjected to multiphase of tectonic movements. The multi trends of paleostress in the directions (EEN – WWS to NNE – SSW) with following direction maximum stress (σ1) (04/256) to (17/195) might be attributed to the oblique collision of the Arabian and Eurasian plates along their zigzag margins, and to the anticlockwise rotation of the Arabian plate relative to Eurasian plate.

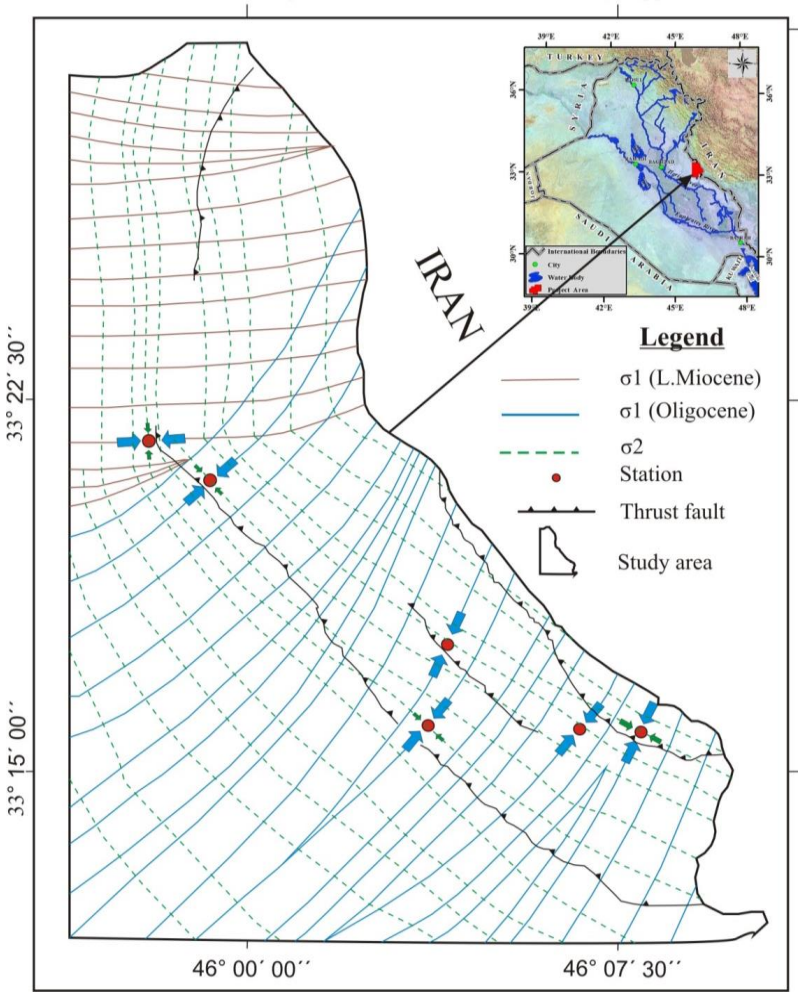

Fig.10: Stress trajectory map of the study area

CONCLUSIONS

The study area was subjected to two main stress fields; the first continued from Oligocene to the Middle Miocene and characterized by NE – SW and NNE – SSW compressions and NW – SE and WNW – ESE extensions. The second stress field started in the Late Miocene and characterized by E – W compression and N – S extension. The area was subjected to multiphase tectonic movements which resulted in multi trends of paleostress in the directions (EEN – WWS to NNE – SSW), which might be attributed to the oblique collision of the Arabian and Eurasian plates and to the anticlockwise rotation of the Arabian Plate relative to the Eurasian Plate.

REFERENCES

Aleksandrowski, P., 1985. Graphical determination of principal stress directions for slickenside lineation populations: An attempt to modify Arthaud's method. Journal of Structural Geology, Vol. 7, p. 73 – 82.

Al-Kadhimi, J.M.A., Sissakian, V.K., Fattah, A.S. and Deikran, D.B., 1996. Tectonic Map of Iraq, scale 1: 1000 000, 2nd edit. GEOSURV, Bagdad.

Al-Kotbah, A.M. and Al-Ubaidi, M.R., 2001. Principal stress orientation of Yemen faults in the Mesozoic age, Sana`a University. Faculty of Science Bull., Vol.14, p. 85 – 103.

Al-Mubarak, M.A. and Youkhanna, R.Y., 1976. Report on the regional geological mapping of Al-Fatah – Mosul Area. GEOSURV, int. rep. no. 753.

Al-Ubaidi, M.R. and Al-Kotbah, A.M., 2003. The Magnitudes of the paleostresses of the Yemen faults in the sedimentary cover. Sana'a unv. Faculty of science Bull. Vol.16, p. 95 – 109.

Anderson, E.M., 1951. The dynamics of faulting and dyke formation with applications to Brittain: Edinburgh, Oliver and Boyd, 206pp.

Angelier, J., 1979. Determination of the mean principal directions of stresses for a given fault population: Tectonophysics, Vol.56, p. T17 – T26.

Angelier, J., 1984. Tectonic analysis of fault slip data sets: Journal of Geophysical Research, Vol.89, p. 5835 – 5848.

Angelier, J., 1985. Extension and rifting: the Zeit region, Gulf of Suez: Journal of Structural Geology, Vol.7, p. 605 – 611.

Angelier, J., 1989. From orientation to magnitudes in paleostress determinations using fault slip data: Journal of Structural Geology, Vol.11, p. 37 – 50.

Angelier, J., Colletta, B. and Anderson, R.E., 1985. Neogene paleostress changes in the Basin and Range: A case study at Hoover Dam, Nevada-Arizona: Geological Society of America Bulletin, Vol.96, p. 347 – 361.

Angelier, J. and Mechler, P., 1977. Sur une methode graphique de recherche des contraintes principales egalment utilisable en tectonique et en seismologie: La methode des diedres droits: Bulletin de Societie Geologique de France, Vol.19, p. 1309 – 1318.

Angelier, J., Tarantola, A., Valette, B., and Manoussis, S., 1982, Inversion of field data in fault tectonics to obtain the regional stress. I., Single phase fault populations: A new method of computing the stress tensor: Geophys. J.R. Astron. Soc., Vol.69, p. 607 – 621.

Angelier, J., 1994. Fault slip analysis and paleostress reconstruction. Continental Deformation, 53 – 100. Oxford: Pergamon Press.

Aydin, A., 1980. Determination of the orientation of the principal stresses from three or more sets of contemporaneous faults (abstract). EOS: Transactions of the American Geophysical Union. Vol.61, 1117pp.

Benkhelil, J., 1989. The origin and evolution of the Cretaceous Benue Trough (Nigeria). Journal of African Earth Sciences (and the Middle East), Vol.8, Nos. 2 – 4, p. 251 – 282.

Bott, M.H.P., 1959. The mechanics of oblique -slip faulting. Geological Magazine. Vol.96, p. 109 – 117.

Buday, T. and Jassim, S.Z., 1987. The Regional Geology of Iraq, Vol.2, Tectonism, Magmatism and Metamorphism. GEOSURV, Baghdad, 352pp.

Caputo, M. and Caputo, R. 1988. Structural analysis: New analytical approach and applications. Annales Tectonicæ. Vol.2, p. 84 – 89.

Célérier, B., 1988. How much does slip on a reactivated fault plane constrain the stress tensor? Tectonics. Vol.7, p. 1257 – 1278.

Delvaux, D., 1993. The TENSOR program for paleostress reconstruction: examples from the east African and the Baikal rift zones. Terra Nova. Vol.5, No.1, 216pp.

Delvaux, D., Moeys, R., Stapel, G., Petit, C., Levi, K., Miroshnichenko, A. and San'kov, V., 1997. Paleostress reconstructions and geodynamics of the Baikal region, Central Asia, Part 2. Cenozoic rifting. Tectonophysics, Vol.282, Nos. 1 – 4, p. 1 – 38.

Delvaux, D. and Sperner, B., 2003. New aspects of tectonic stress inversion with reference to the TENSOR program. Geological Society, London, Special Publications, Vol.212, No.1, p. 75 – 100.

Etchecopar, A., Vasseur, G. and Daignieres, M., 1981. An inverse problem in microtectonics for the determination of stress tensors from fault striation analysis . Journal of Structural Geology. Vol.3, p. 51 – 65.

Fouad, S.F.A., 2012. Western Zagros Fold-Thrust Belt, Part I. The Low Folded Zone. Iraqi Bull. Geol. Min., Special Issue, No.5, p. 39 – 62.

Frizzell, V.A. and Zoback, M.L., 1987. Stress orientation determined from fault slip data in Hampel Washarea, Nevada, and its relation to contemporary regional stress field. Tectonics. Vol.6, p. 89 – 98.

Guiraud, M., Laborde, O. and Philip, H., 1989. Characterization of various types of deformation and their corresponding deviatoric stress tensors using microfault analysis. Tectonophysics Vol.170, p. 289 – 316.

Hancock, P.L., Al-Kahdi, A., Barka, A.A. and Bevan, T.G., 1987. Aspects of analyzing Brittle structures . Annales Tectonicæ. Vol.1, p. 5 – 19.

Hancock, PL., 1985. Brittle microtectonics: principles and practice. Journal of Structural Geology. Vol.7, p. 437 – 457.

Hardcastle, K.C., 1989. Possible paleostress tensor configurations derived from fault – slip data in eastern Vermont and western New Hampshire. Tectonics. Vol.8, p. 265 – 284.

Hatzor, Y. and Reches, Z., 1990. Structure and paleostresses in the Gilboaregion, western margins of the Dead Sea transform. Tectonophysics. Vol.180, p. 87 – 100.

Igwe, O. and Okonkwo, I.A., 2016. Application of paleostress analysis for the identification of potential instability precursors within Benue Trough Nigeria. Geoenvironmantal disasters. Vol.3, p. 2 – 15.

Jaeger, J.C., 1969. Elasticity , Fracture and Flow. 2nd edit. Methuen: London. 268pp.

Jassim, S.Z. and Goff, J.C., 2006. Geology of Iraq. Prague and Moravian Museum, Brno, 341pp.

Julien, P. and Cornet, F., 1987. Stress determination from aftershocks of the Campania – Lucania earthquake of November 23, 1980. Annales Geophysicæ. Vol.5B, p. 289 – 300.

Larroque, J.M. and Laurent, P., 1988. Evolution of the stress field pattern in the south of the Rhine Graben from the Eocene to the present. Tectonophysics. Vol.148, p. 41 – 58.

Lisle, R.J., 1987. Principal stress orientations from faults: An additional constraint. Annales Tectonicæ. Vol.1, p. 155 – 158.

Lisle, R.J., 1988. ROMSA: A BASIC program for paleostress analysis using fault – striation data. Computers and Geosciences. Vol.14, p. 255 – 259.

Ma'ala, Kh.A., Fouad, S.A., Lawa, F.A., Philip, W. and Al-Hassny, N., 1987. Report on the geological investigation for northern sector of the Fatha– Mosul Sulfur District. GEOSURV, int. rep. no. 1935.

Mahmoud, A.A., Ali, M.A., Mohammed, A.J., Al-Mikhtar, L.E., Al-kubaysi, K.N., Hussien, M.S., Al-Obaidy, R.A., Mohammed Ali, S.M., Tawfeeq, G., Jassim, M.K., Shnaen, S.R. and Kareem, A.Y., 2018. Detailed geological mapping of Iraq, Zurbatiyah region, east Iraq, scale 1: 250 000. GEOSURV, int. rep. no. 3650.

Manning, A.H. and de Boer, J.Z., 1989. Deformation of Mesozoic dikes in New England. Geology. Vol.17, p. 1016 – 1019.

Marzouk, I.M. and Sattar, M.A., 1994. Wrench tectonic in Abu Dhabi, UAE, the Middle East Geosciences Exhibition and Conference, Bahrain, April, p. 25 – 27.

Michael, A.J., 1984. Determination of stress from slip data: Fault sand folds. Journal of Geophysical Research. Vol.89, p. 517 – 526.

Park, R.G., 1997. Foundation of Structural Geology, 3rd edit. Chapman and Hall, London, 202pp.

Pfiffner, O.A. and Burkhard, M., 1987. Determination of paleo-stress axes orientations from fault, twin and earthquake data. Annales Tectonicæ. Vol.1, p. 48 – 57.

Ramsay, J.G. and Lisle, R.J., 2000. Applications of Continuum Mechanics in Structural Geology. Techniques of modern structural geology. Vol.3. Techniques of modern structural geology, London: Academic Press.

Sassi, W. and Carey-Gailhardis, E., 1987. Interprétation méchanique de glissementsur les failles: Introduction duncritère de frottement. Annales Tectonicæ. Vol.1, p. 139 – 154.

Reches, Z., 1987. Determination of the tectonic stress tensor from slip a long faults that obey the Coulomb yield condition. Tectonics. Vol.6, p. 849 – 861.

Wallace, R.E., 1951. Geometry of shearing stress and relation to faulting. Journal of Geology. Vol.59, p.118 – 130.

Wallbrecher, E. and Fritz, H., 1989. Quantitative evaluation of the shape factor and the orientation of a paleo-stress ellipsoid from the distribution of slickenside striations. Annales Tectonicæ. Vol.3, p. 110 – 122.

Yacoub, S.Y., Othman, A.A. and Kadim, T.H., 2012. Geomorphology of the Low Folded Zone. Iraqi Bull. Geol. Min., Special Issue, No.5, p. 7 – 37.